Functional Nanoparticles

DOI: 10.1002/ange.201306724

Functional Iron Oxide Magnetic Nanoparticles with Hyperthermia-Induced Drug Release Ability by Using a Combination of Orthogonal Click Reactions**

*Thuy T. T. N'Guyen, Hien T. T. Duong, Johan Basuki, Véronique Montembault, Sagrario Pascual, Clément Guibert, Jérôme Fresnais, Cyrille Boyer, Michael R. Whittaker, Thomas P. Davis, and Laurent Fontaine**

Magnetic iron oxide nanoparticles (IONPs) are under investigation for several biomedical applications,[1] including drug delivery,[2] magnetic resonance imaging (MRI),[3] and hyperthermia therapy.[4] Indeed, the application of an external alternating magnetic field (AMF) to IONPs induces production of thermal energy, by Neel and/or Brownian relaxation, that can be used to generate local heating for tumor repression.[4,5] IONPs have been also proposed as controlled delivery systems in which remote release of suitable therapeutic agents is stimulated by the heat generated upon AMF exposure.[5,6] In the design of ligands that allow simple and efficient functionalization of IONPs with a desired moiety, cycloaddition reactions are ideal candidates. Cycloadditions have received broad attention because these orthogonal click-type reactions can be efficiently used for bioconjugation.[7] Additionally, cycloadditions are chemoselective and may be efficiently performed under physiological conditions, both in vitro and in vivo.[7] The 1,3-dipolar azide–alkyne click reaction has found widespread applications in materials science and bioconjugation, as either copper-catalyzed (CuAAC) or strain-promoted azide–alkyne cycloaddition.[8] The Diels–Alder (DA) reaction is known as a thermoreversible reaction between diene and alkene derivatives (dienophiles) to form cycloadducts in a clean and simple click reaction that is effective in aqueous conditions.[9] Owing to these desirable features, both cycloadditions have been widely employed in a variety of materials synthesis applications, including IONP functionalization.[1,8,10,11] While IONPs have been functionalized with a single type of functional group by using either Diels–Alder[10] or 1,3-dipolar cycloaddition click reactions,[11] there are no examples where both have been applied.

Herein, we report on the design and preparation of a new class of functional IONP by using a versatile methodology that employs a combination of orthogonal click reactions: CuAAC and thermoreversible DA. We designed a versatile multifunctional ligand that contains a phosphonic acid group, which is known to strongly bind to the iron oxide surface of IONPs,[11,12] and two orthogonal clickable groups: an alkyne moiety for installing an azide end-functionalized hydrophilic polymer through 1,3-dipolar cycloaddition to impart aqueous dispersability/stability, antifouling property, and biocompatibility to the IONPs; and a furan ring that serves as a thermoreversible linker for a biologically active molecule (or probe) through reversible DA chemistry (Scheme 1).

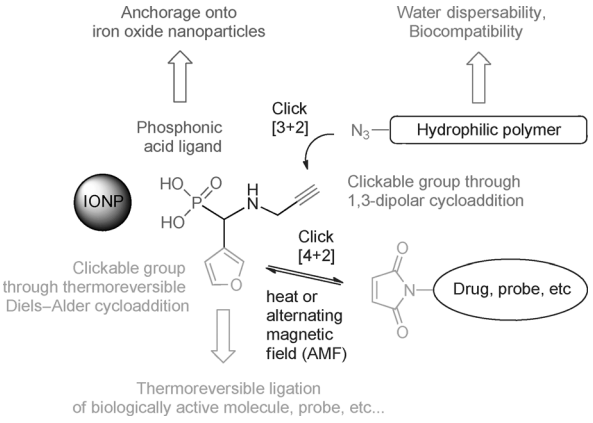

Scheme 1. Multifunctional ligand with orthogonal clickable groups.

We speculated that upon AMF exposure, such functional IONPs would release the biologically active or probe payload through retro-DA (rDA) reactions. While rDA reactions generally proceed at temperatures that are not compatible with biological applications (90–110 °C), we hypothesized that using this approach, sufficient energy could be brought in

[*] Dr. T. T. T. N'Guyen, Dr. V. Montembault, Dr. S. Pascual, Prof. Dr. L. Fontaine
Institut des Molécules et des Matériaux du Mans
UMR 6283—Equipe Méthodologie et Synthèse des Polymères
CNRS—Université du Maine
Avenue Olivier Messiaen, 72085 Le Mans Cedex (France)
E-mail: laurent.fontaine@univ-lemans.fr
H. T. T. Duong, J. Basuki, Assoc. Prof. Dr. C. Boyer
Australian Centre for Nanomedicine, Sydney (Australia)
Dr. M. R. Whittaker, Prof. Dr. T. P. Davis
Monash Institute of Pharmaceutical Sciences
Melbourne (Australia)
C. Guibert, Dr. J. Fresnais
PECSA, UMR 7195, Laboratoire de Physico-Chimie des Electrolytes, Colloïdes et Sciences Analytiques, Paris (France)

[**] We thank Dr. S. Piogé and Prof. Dr. F. Goutenoire for TEM analyses, A. Durand and E. Mebold for NMR and MALDI-TOF analyses, A. McMillan and R. Whan for FLIM experiments, and Dr. G. Dujardin for helpful discussions. C.B. is thankful for his APD and Future Fellowship from Australian Research Council (ARC).

Supporting information (including experimental details) for this article is available on the WWW under http://dx.doi.org/10.1002/anie.201306724.

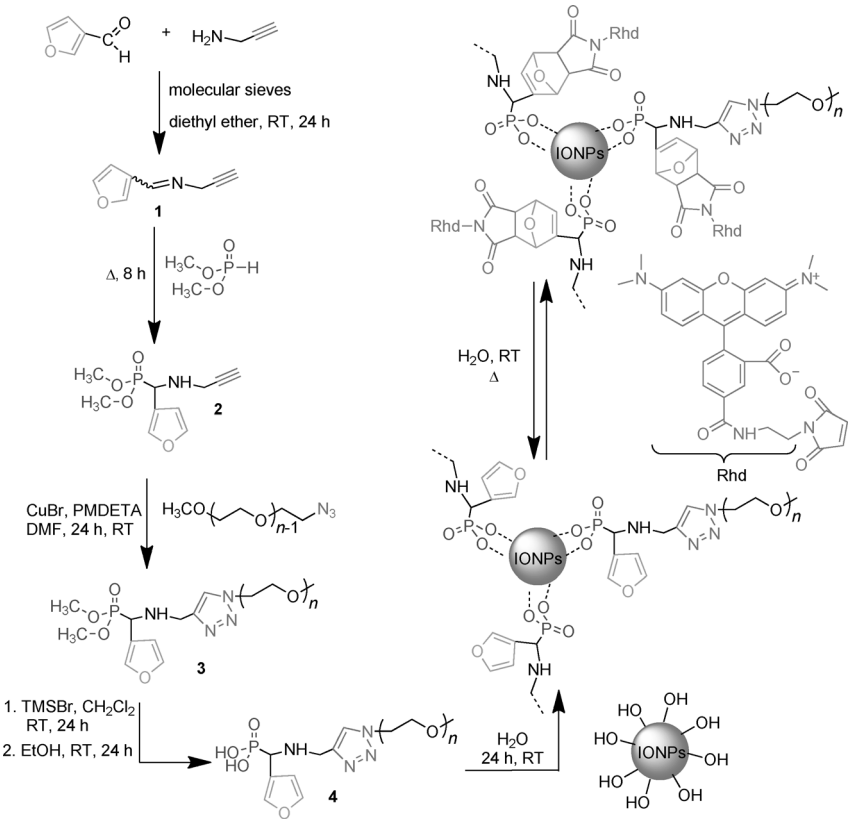

Scheme 2. Multistep synthesis of IONPs coated with furan-functionalized phosphonic acid terminated PEO and subsequent Rhd loading. PMDETA = *N*,*N*,*N*′,*N*″,*N*″-pentamethyldiethylenetriamine, DMF = *N*,*N*-dimethylformamide, TMS = trimethylsilyl.

close proximity to the cycloadduct to initiate the rDA reaction without more delocalized overheating. Herein, we report the proof-of-principle of this concept.

To test our hypothesis, we prepared functional IONPs according to Scheme 2. The IONPs were first synthesized through a coprecipitation method.[13] A typical transmission electron microscopy (TEM) image of the IONPs obtained is shown in Figure S1A in the Supporting Information. The IONPs have an average size of 13.0 ± 1.0 nm. The average size, estimated from the iron oxide (311) peak in the X-ray diffraction pattern of IONPs by using the Scherrer equation, is 10.4 ± 0.3 nm, close to the value from the TEM images.

To stabilize and functionalize the IONPs, a phosphonic acid terminated furan-functionalized poly(ethylene oxide) (PEO) monomethyl ether (**4**) was prepared by combining a Kabachnik–Fields[14] reaction with CuAAC chemistry, thus introducing a furanyl functionality and a phosphonic acid group, respectively, at the chain-end of PEO monomethyl ether (Scheme 2 and the Supporting Information).[15] Briefly, *N*-(3-furanylmethylene)prop-2-yn-1-amine (**1**) was reacted with dimethyl hydrogen phosphonate to afford [*N*-methyl-(dimethoxyphosphonyl)(3-furanyl)]prop-2-yn-1-amine (**2**), which was then used for a typical CuAAC with azide terminated PEO monomethyl ether. The resultant dimethylphosphonate-terminated furan-functionalized PEO monomethyl ether **3** was then converted into its phosphonic acid homologue **4** by dealkylation.[15]

The feasibility of DA and rDA reactions between the furan group of **4** and *N*-methylmaleimide, which was used as a model for maleimide-functionalized cargo, was then investigated (Scheme S5). Successful conjugation in D_2O at 40 °C was demonstrated by ^{1}H NMR spectroscopy. Based on ^{1}H NMR (Figure S18B), the conjugation gave a conversion of 85 %. The rDA reaction occurred in D_2O at 80 °C with 71 % efficiency after 48 h of reaction, as ascertained from the ^{1}H NMR spectrum (Figure S18C).

Compound **4** was then grafted onto IONPs by using the strong affinity of the terminal phosphonic acid for iron oxide surfaces, thereby yielding IONPs@**4** (Scheme 2). The surface chemistry of the IONPs@**4** was assessed by Fourier transform infrared-attenuated total reflectance (FTIR-ATR; Figure S19B) and X-ray photoelectron spectroscopy (XPS; Figures S20–S22). Thermogravimetric analysis (TGA) showed that the amount of **4** on IONPs@**4** was about 13 % of the total particle weight, as determined from the significant mass change between 250 and 400 °C owing to decomposition of **4** (Figure S23B). The grafting density, calculated using the weight loss and the specific surface area of the IONPs (equation in the Supporting Information), was estimated to be 0.20 chain per nm^2, a density consistent with a grafting-onto approach. The stability of the IONPs@**4** was examined under biologically relevant conditions. When incubating the IONPs@**4** in phosphate buffer (pH 7.4) containing bovine serum albumin (BSA) at increasing concentrations (0.02–0.2 g L^{-1}) at 25 °C for 24 h, the average particle size was not affected by the increasing concentration of BSA (Figure S24).

To investigate the potential application of these novel coated IONPs for drug delivery, tetramethylrhodamine-5-C2-maleimide (Rhd-M, 1.8 mmol L^{-1}) was loaded as a fluorescence probe and model drug within the IONPs@**4** by DA reaction conducted in pure water at 40 °C over 14 days (Scheme S6). Fluorescence lifetime imaging microscopy (FLIM) was used to determine the lifetimes of free Rhd-M and IONPs@Rhd by using time-correlated single photon counting (TCSPC; see the Supporting Information). The concentration-independent decay was fitted to a single exponential with a resulting fluorescence lifetime (τ) of 2 ns for free Rhd-M (Figure 1). It is noted that there is a significant amount of unreacted free dye in the sample (fluorescence lifetime τ of 2 ns) before the purification; as can be seen in the lifetime distribution, the average τ is unchanged. However, after purification by dialysis to remove the free dye, it can be seen that the fluorescence lifetime of the dye decreases (2 ns to 1.6 ns, see Figure 1). This decrease in fluorescence lifetime is attributed to a fluorescence quenching effect owing to very close proximity of conjugated Rhd dye to the iron oxide core.

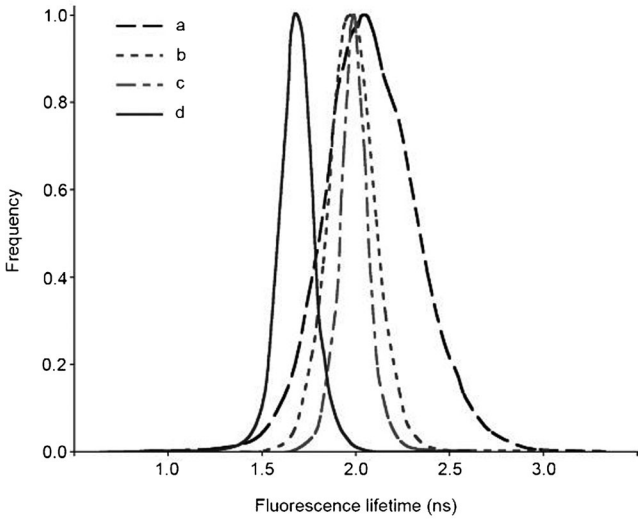

Figure 1. Fluorescence lifetime distribution of the mixture issued after 48 h from the rDA reaction of IONPs@Rhd at 70 °C in the presence of NaCl (a); Rhd-M (b); and IONPs@Rhd issued from the DA reaction between IONPs@**4** and Rhd-M both before (c) and after (d) purification by dialysis.

These data confirm the quenching effect of fluorophores in proximity to the IONPs that has been reported and can be explained by radiative energy transfer between the dye and iron oxide or the collision of dye and IONPs.[16] The release of the dye from conjugated IONPs was investigated by using a thermal rDA reaction at 70 °C over 48 h. When the dye is cleaved from the core by rDA reaction, it is then free to diffuse away from the iron oxide core: the fluorescent quenching effects are removed and the fluorescence lifetime is restored.[17] Interestingly, in aqueous solution, the dyes were still in proximity to the IONPs after the rDA reaction, as evident from the unchanged lifetime distribution (data not shown, lifetime 1.6 ns). We attributed this to the binding of the free dye to the IONPs through charge–charge interactions. We speculated that the presence of charged ions added to the solution (namely NaCl) would disrupt this electrostatic binding and free the dye, thus restoring the longer fluorescent lifetime as the dye moves away from the core and fluorescent quenching effects are minimized.[17] In the presence of 0.1 M NaCl aqueous solution, which mimics the concentration of sodium chloride in blood plasma, only the contribution of a longer lifetime signal (average 2 ns) was observed (Figure 1), a result consistent with the successful release of the dye from the IONP cores.

Recent results have shown that localized heating is observed when IONPs are excited by AMF but no macroscopic temperature increase is detected. Huang et al.[18] demonstrated that the cell membrane could be heated while the Golgi apparatus did not experience a temperature increase. While studying the effects of IONPs and AMF on membrane opening and fluorophore release, Creixell et al.[19] also demonstrated that no macroscopic temperature increase was evident. The effect of magnetic hyperthermia induces a high temperature gradient from the nanoparticle surface; this gradient is restricted to the environment close to the periphery of the nanoparticle, from a few angstroms to less than a nanometer scale, thus leading to localized heating.[20] Our ligand **4** has been precisely designed to provide a cleavable bond very close to the nanoparticle surface. Exciting the magnetic moments of the nanoparticles should bring enough energy to engage the rDA reaction. However, applying efficient hyperthermia to induce bond cleavage requires optimization of the magnetic field frequency together with the size of the IONPs.[21] We thus used a size-sorted maghemite ferrofluid (Figures S2–S5 and Table S1) obtained according to the method described by Massart et al.[22] IONPs@Rhd were synthesized using a grafting-onto strategy. The resulting IONPs@Rhd were precipitated, redispersed, and dialyzed to ensure the removal of all traces of free ligand. UV/Vis spectra were used both to determine iron oxide concentration (in the UV range) and to confirm the presence of the Rhd-labeled ligand on the nanoparticles (band centered at 552 nm). Comparison of iron oxide and Rhd concentrations obtained after fluorescence calibration gave a grafting density of 0.76 Rhd nm^{-2}. Specific loss power of uncoated size-sorted nanoparticles was obtained for a 7.6 wt% ferrofluid at 332.5 kHz and 11.3 kA m^{-1} field, giving 49 W g^{-1}, a result in good agreement with theoretical and experimental expectations;[21] at this concentration and under these excitation conditions, we obtained a temperature increase rate of 0.88 °C s^{-1}. This means that using these nanoparticles at this concentration would increase the medium temperature from 30 °C to 80 °C in less than one minute. Under these conditions, deconvoluting the nanoparticle heating properties from macroscopic heating effects is nontrivial. To decouple the rDA reaction from any global temperature increase, the IONPs@Rhd dispersion was diluted down to 2.5×10^{-3} and 2.5×10^{-2} wt%. This would only give a temperature increase of 0.0014 °C and 0.014 °C every minute, respectively, an increase not sufficiently large to increase the medium temperature. However, a slight macroscopic temperature increase could still be contributed by eddy currents (owing to the presence of salt in the solution) or by heating of the metal wire. In consideration of these caveats, no significant temperature increase was detected during nanoparticle excitation (Figure S25). Samples were prepared and placed under hyperthermia excitation for periods of 2, 5, 10, and 27.5 min. Samples were then centrifuged (at 5000 rpm for 30 min) on a 10 kD membrane to recover the supernatant. The fluorescence of the supernatant was measured using a calibration curve (Figure S26A) for comparison to the fluorescence of the supernatant of untreated samples at a defined concentration. Notably, a sample left for 22 min at (29 ± 1) °C, which is the temperature of the magneTherm measurement cell, did not show any significant Rhd release (Figure S26B). The control experiment without AMF exposure showed only a little Rhd liberation. By contrast, nanoparticles treated with AMF released 3 nM (2 min at 2.5×10^{-3} wt%) to 105 nM (10 min at 2.5×10^{-2} wt%) of Rhd (Figure 2); concentration values that fall within the range of IC_{50} values for many anticancer drugs.[23] The rDA reaction thus occurs close to the IONP surface as a result of AMF-induced excitation. Given the ability of tumors to preferentially accumulate nanoparticles,[24] these results demonstrate

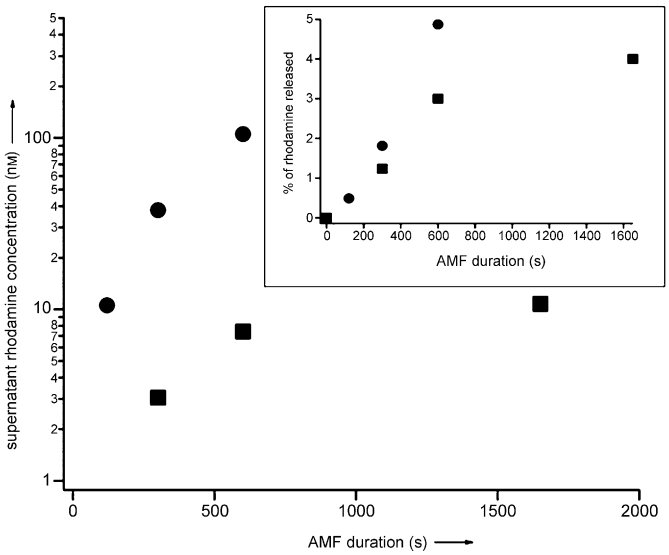

Figure 2. Concentration of Rhd released against AMF duration. Inset: percent of the Rhd released normalized by the initial concentration against treatment duration (■ 2.5×10^{-3}%wt; ● 2.5×10^{-2}%wt).

that such a drug delivery system could be useful in hyperthermia-induced drug delivery applications. Interestingly, the reaction kinetics of the rDA reaction are similar at the two concentrations used (Figure 2 inset: same slope of Rhd release in %).

In summary, we report a method for the production of novel functional IONPs showing unprecedented, active control over drug release by rDA reaction by using hyperthermia effects. Our synthetic design, which is based on a versatile multifunctionalization of IONPs, allows us to control the release of the conjugated drug whilst maintaining the colloidal stability and magnetic properties of the IONPs. Upon AMF exposure, the rDA reaction enables the release of the conjugated drug without any significant heating of the medium. This method has the potential to improve hyperthermia therapies by expanding the range of polymers and molecules (drugs, dyes, etc) that can be used. This class of functional IONPs may become important theranostic tools for preparing the next generation of controlled-release devices and nanomedicines for in vitro and in vivo applications.

Received: August 1, 2013
Revised: September 24, 2013
Published online: November 19, 2013

Keywords: click chemistry · controlled release · drug delivery · iron oxide nanoparticles · retro-Diels–Alder reaction

[1] For recent a book and reviews, see: a) T. K. T. N'Guyen, *Magnetic Nanoparticles: From Fabrication to Clinical Applications*, CRC, Boca Raton, FL, **2012**; b) Z. L. Cheng, A. Al Zaki, J. Z. Hui, V. R. Muzykantov, A. Tsourkas, *Science* **2012**, *338*, 903–910; c) L. H. Reddy, J. L. Arias, J. Nicolas, P. Couvreur, *Chem. Rev.* **2012**, *112*, 5818–5878; d) E. Amstad, M. Textor, E. Reimhult, *Nanoscale* **2011**, *3*, 2819–2843; e) R. Hao, R. J. Xing, Z. C. Xu, Y. L. Hou, S. Gao, S. H. Sun, *Adv. Mater.* **2010**, *22*, 2729–2742; f) C. Boyer, M. R. Whittaker, V. Bulmus, J. Q. Liu, T. P. Davis, *NPG Asia Mater.* **2010**, *2*, 23–30; g) J. H. Gao, H. W. Gu, B. Xu, *Acc. Chem. Res.* **2009**, *42*, 1097–1107; h) N. A. Frey, S. Peng, K. Cheng, S. H. Sun, *Chem. Soc. Rev.* **2009**, *38*, 2532–2542; i) S. Laurent, D. Forge, M. Port, A. Roch, C. Robic, L. V. Elst, R. N. Muller, *Chem. Rev.* **2008**, *108*, 2064–2110; j) A. H. Lu, E. L. Salabas, F. Schuth, *Angew. Chem.* **2007**, *119*, 1242–1266; *Angew. Chem. Int. Ed.* **2007**, *46*, 1222–1244.

[2] a) V. I. Shubayev, T. R. Pisanic, S. H. Jin, *Adv. Drug Delivery Rev.* **2009**, *61*, 467–477; b) D. Ho, X. L. Sun, S. H. Sun, *Acc. Chem. Res.* **2011**, *44*, 875–882; c) S. Mura, P. Couvreur, *Adv. Drug Delivery Rev.* **2012**, *64*, 1394–1416.

[3] a) N. Lee, T. Hyeon, *Chem. Soc. Rev.* **2012**, *41*, 2575–2589; b) S. Jiang, K. Y. Win, S. H. Liu, C. P. Teng, Y. G. Zheng, M. Y. Han, *Nanoscale* **2013**, *5*, 3127–3148; c) H. Mok, M. Q. Zhang, *Expert Opin. Drug Delivery* **2013**, *10*, 73–87.

[4] a) B. Hildebrandt, P. Wust, O. Ahlers, A. Dieing, G. Sreenivasa, T. Kerner, R. Felix, H. Riess, *Crit. Rev. Oncol. Hematol.* **2002**, *43*, 33–56; b) C. Kumar, F. Mohammad, *Adv. Drug Delivery Rev.* **2011**, *63*, 789–808; c) S. Laurent, S. Dutz, U. O. Hafeli, M. Mahmoudi, *Adv. Colloid Interface Sci.* **2011**, *166*, 8–23; d) J. H. Lee, J. T. Jang, J. S. Choi, S. H. Moon, S. H. Noh, J. W. Kim, J. G. Kim, I. S. Kim, K. I. Park, J. Cheon, *Nat. Nanotechnol.* **2011**, *6*, 418–422.

[5] a) J. Dobson, *Nat. Nanotechnol.* **2008**, *3*, 139–143; b) D. Yoo, H. Jeong, C. Preihs, J. S. Choi, T. H. Shin, J. L. Sessler, J. Cheon, *Angew. Chem.* **2012**, *124*, 12650–12653; *Angew. Chem. Int. Ed.* **2012**, *51*, 12482–12485.

[6] a) S. Mornet, S. Vasseur, F. Grasset, E. Duguet, *J. Mater. Chem.* **2004**, *14*, 2161–2175; b) A. K. Gupta, M. Gupta, *Biomaterials* **2005**, *26*, 3995–4021.

[7] a) E. M. Sletten, C. R. Bertozzi, *Angew. Chem.* **2009**, *121*, 7108–7133; *Angew. Chem. Int. Ed.* **2009**, *48*, 6974–6998; b) Z. Hao, S. Hong, X. Chen, P. R. Chen, *Acc. Chem. Res.* **2011**, *44*, 742–751; c) J. Dommerholt, S. Schmidt, R. Temming, L. J. A. Hendriks, F. P. J. T. Rutjes, J. C. M. van Hest, D. J. Lefeber, P. Friedl, F. L. van Delft, *Angew. Chem.* **2010**, *122*, 9612–9615; *Angew. Chem. Int. Ed.* **2010**, *49*, 9422–9425.

[8] a) H. C. Kolb, M. G. Finn, K. B. Sharpless, *Angew. Chem.* **2001**, *113*, 2056–2075; *Angew. Chem. Int. Ed.* **2001**, *40*, 2004–2021; b) J. F. Lutz, Z. Zarafshani, *Adv. Drug Delivery Rev.* **2008**, *60*, 958–970; c) M. F. Debets, S. S. Van Berkel, J. Dommerholt, A. J. Dirks, F. Rutjes, F. L. Van Delft, *Acc. Chem. Res.* **2011**, *44*, 805–815; d) J. Lahann, *Click Chemistry for Biotechnology and Materials Science*, Wiley, Chichester, **2009**.

[9] a) J. M. Palomo, *Eur. J. Org. Chem.* **2010**, 6303–6314; b) M. A. Tasdelen, *Polym. Chem.* **2011**, *2*, 2133–2145.

[10] P. Riente, J. Yadav, M. A. Pericas, *Org. Lett.* **2012**, *14*, 3668–3671.

[11] a) M. A. White, J. A. Johnson, J. T. Koberstein, N. J. Turro, *J. Am. Chem. Soc.* **2006**, *128*, 11356–11357; b) P. C. Lin, S. H. Ueng, S. C. Yu, M. D. Jan, A. K. Adak, C. C. Yu, C. C. Lin, *Org. Lett.* **2007**, *9*, 2131–2134; c) L. Qi, A. Sehgal, J. C. Castaing, J. P. Chapel, J. Fresnais, J. F. Berret, F. Cousin, *ACS Nano* **2008**, *2*, 879–888; d) D. Toulemon, B. P. Pichon, X. Cattoen, M. W. C. Man, S. Begin-Colin, *Chem. Commun.* **2011**, *47*, 11954–11956; e) S. Kinge, T. A. Gang, W. J. M. Naber, W. G. van der Wiel, D. N. Reinhoudt, *Langmuir* **2011**, *27*, 570–574; f) E. Guénin, J. Hardouin, Y. Lalatonne, L. Motte, *J. Nanopart. Res.* **2012**, *14*, 965–975.

[12] a) C. Boyer, V. Bulmus, P. Priyanto, W. Y. Teoh, R. Amal, T. P. Davis, *J. Mater. Chem.* **2009**, *19*, 111–123; b) C. Boyer, P. Priyanto, T. P. Davis, D. Pissuwan, V. Bulmus, M. Kavallaris, W. Y. Teoh, R. Amal, M. Carroll, R. Woodward, T. St Pierre, *J. Mater. Chem.* **2010**, *20*, 255–265; c) T. J. Daou, J. M. Greneche, G. Pourroy, S. Buathong, A. Derory, C. Ulhaq-Bouillet, B.

Donnio, D. Guillon, S. Begin-Colin, *Chem. Mater.* **2008**, *20*, 5869 – 5875.
[13] J. Basuki, L. Essers, P. B. Zetterlund, M. R. Whittaker, C. Boyer, T. P. Davis, *Macromolecules* **2013**, *46*, 6038 – 6047.
[14] a) M. I. Kabachnik, T. Y. Medved, *Dokl. Akad. Nauk SSSR* **1952**, *83*, 689 – 692 [*Chem. Abstr.* **1953**, *47*, 2724b]; b) E. K. Fields, *J. Am. Chem. Soc.* **1952**, *74*, 1528 – 1531; c) L. Ménard, L. Fontaine, J. C. Brosse, *React. Polym.* **1994**, *23*, 201 – 212; d) N. S. Zefirov, E. D. Matveeva, *ARKIVOC* **2008**, 1 – 17.
[15] T. T. T. N'Guyen, K. Oussadi, V. Montembault, L. Fontaine, *J. Polym. Sci. Part A* **2013**, *51*, 415 – 423.
[16] a) S. Liu, R. Xing, F. Lu, R. K. Rana, J. J. Zhu, *J. Phys. Chem. C* **2009**, *113*, 21042 – 21047; b) H. Qu, D. Caruntu, H. Liu, C. J. O'Connor, *Langmuir* **2011**, *27*, 2271 – 2278; c) J. Lakowicz, *Principles of Fluorescence Spectroscopy*, Springer, New York, **2006**.
[17] Y. Wang, B. Li, L. Zhang, P. Li, J. Zhang, *Langmuir* **2012**, *28*, 1657 – 1662.
[18] H. Huang, S. Delikanli, H. Zeng, D. M. Ferkey, A. Pralle, *Nat. Nanotechnol.* **2010**, *5*, 602 – 606.
[19] M. Creixell, A. C. Bohorquez, M. Torres-Lugo, C. Rinaldi, *ACS Nano* **2011**, *5*, 7124 – 7129.
[20] A. Riedinger, P. Guardia, A. Curcio, M. A. Garcia, R. Cingolani, L. Manna, T. Pellegrino, *Nano Lett.* **2013**, *13*, 2399 – 2406.
[21] J. P. Fortin, C. Wilhelm, J. Servais, C. Ménager, J. C. Bacri, F. Gazeau, *J. Am. Chem. Soc.* **2007**, *129*, 2628 – 2635.
[22] R. Massart, E. Dubois, V. Cabuil, E. Hasmonay, *J. Magn. Magn. Mater.* **1995**, *149*, 1 – 5.
[23] For example, doxorubicin shows $IC_{50} = 36$ nM against S5Y5 cells, see: H. T. T. Duong, F. Hughes, S. Sagnella, M. Kavallaris, A. McMillan, R. Whan, J. Hook, T. P. Davis, C. Boyer, *Mol. Pharm.* **2012**, *9*, 3046 – 3061; while 26-fluoroepothilone B against human prostate cancer cells has an $IC_{50} = 0.5$ to 4 nM, see: R. A. Newman, J. Yang, M. R. V. Finlay, F. Cabral, D. Vourloumis, L. C. Stephens, P. Troncoso, X. Wu, C. J. Logothetis, K. C. Nicolaou, N. M. Navone, *Cancer Chemother. Pharmacol.* **2001**, *48*, 319 – 326.
[24] M. Wang, M. Thanou, *Pharmacol. Res.* **2010**, *62*, 90 – 99.